Atmos. Chem. Phys. Discuss., 4, 1119–1150, 2004
www.atmos-chem-phys.org/acpd/4/1119/
SRef-ID: 1680-7375/acpd/2004-4-1119

Atmospheric Chemistry and Physics Discussions

Passenger aircraft project CARIBIC 1997–2002, Part II: the ventilation of the lowermost stratosphere

A. Zahn[1], **C. A. M. Brenninkmeijer**[2], **and P. F. J. van Velthoven**[3]

[1]Institute of Meteorology and Climate Research, Karlsruhe, Germany
[2]Max-Planck-Institute for Chemistry, Mainz, Germany
[3]Royal Netherlands Meteorological Institute (KNMI), De Bilt, The Netherlands

Received: 16 December 2003 – Accepted: 5 February 2004 – Published: 16 February 2004

Correspondence to: A. Zahn (andreas.zahn@imk.fzk.de)

Abstract

In Part II of this study, O_3 and CO data collected onboard passenger aircraft at 9–12 km altitude (project CARIBIC) are analysed with respect to downward propagation of stratospheric ozone through the lowermost stratosphere (LMS) and in-mixing of tropospheric air into the LMS. Throughout the LMS ozone undergoes a well-known sine seasonal variation. The amplitude maximum thereof shifts from mid-winter at the 380–400 K isentropic iso-surfaces to typically June around the tropopause. Over the same altitude range, ozone decreases by almost a factor of 10, but the relative amplitude of the seasonal variation steadily increases from ∼10% to ∼40%. This vertically changing seasonality is shown to be due to seasonal downward propagation of stratospheric O_3, modified owing to dilution by in-flowing O_3-poor tropospheric air. This in-mixing of tropospheric air shows the following features: (i) its influence certainly decreases with increasing distance above the tropopause, (ii) its influence maximises in autumn, (iii) it occurs almost exclusively on isentropic iso-surfaces, and (iv) it causes a well-ventilated tropopause transition layer which reaches ∼2 km into the LMS. The turnover time of this tropopause transition layer is in the order of weeks, which we primarily estimate on the basis of the vertically changing seasonal variation of O_3. The observed surprisingly weak spatial inhomogeneity of the mixing layer demonstrates that extratropical cross-tropopause exchange is not controlled by local processes such as the instantaneous synoptic condition, but is controlled by large-scale processes. Our data thus confirm theoretical studies which view stratosphere-troposphere exchange as part of the general atmospheric circulation. Finally, a cross-tropopause O_3 flux of $3.4 + 2.4 \cdot \sin[2\pi \cdot (\mathrm{DayOfYear} - 30)/365]$ in 10^{10} molecules $\mathrm{cm}^{-2}\,\mathrm{s}^{-1}$ is inferred as a lower estimate.

1 Introduction

The lowermost stratosphere (LMS) is referred to as that part of the stratosphere that is accessible from the troposphere via transport along isentropic surfaces (Hoskins, 1991; Holton et al., 1995). Its upper boundary is the 380–400 K isentropic iso-surface and its lower boundary is the tropopause. The individual influence of the two adjoining compartments (overworld and troposphere) on the LMS chemical composition is assumed to vary conspicuously with season. First, overworld and troposphere have a contrasting chemical composition. Second, the permeability of the two transition layers, i.e. the 380–400 K isentropic iso-surface and the tropopause, is known to vary considerably and differently throughout the year (Haynes and Shuckburgh, 2000). Therefore, the chemical composition of the LMS will undergo a strong seasonal cycle. Indeed, balloon-borne measurements of CFC and water vapour in the LMS by Ray et al. (1999) suggest that the LMS primarily contains in spring air characteristic for the overworld, however in autumn air being recently imported from the troposphere.

Besides this qualitative picture, the dynamical complexity of the LMS and the scarcity of spatially and temporally highly resolved tracer data (Emmons et al., 2000) have prevented a quantitative understanding of the ventilation of the LMS. Crucial parameters such as the (seasonally varying) turnover time of the LMS or (bi-directional) trace gas fluxes across the LMS boundaries are still badly quantified.

In the following, well-demonstrated features and the major uncertainties are briefly contrasted:

(i) Stratospheric air descends from the 380 K surface (there peaking in mid-winter) through the LMS and reaches the extratropical tropopause in spring, inferred from tracer data (e.g. Logan, 1999b) as well as meteorological data (e.g. Appenzeller et al., 1996). Badly quantified are the tracer fluxes through the LMS (Lelieveld and Dentener, 2000; McLinden et al., 2000; Olsen et al., 2001, 2002; and references therein), the exact seasonal variation of these tracer fluxes, the difference to the seasonal variation of the flux of mass, and where and due to what processes the final (irreversible) mixing

with tropospheric air actually occurs. For instance, Lagrangian-type trajectory models using ECMWF data (Wernli et al., 2002; Sprenger and Wernli, 2003; Stohl et al., 2003; and references therein) suggest peaking stratosphere-to-troposphere air mass transport in winter, whereas tracer data following the stratospheric bomb tests in the 50s and 60s found peaking fallout debris of stratospheric origin in spring at the surface (e.g. Junge, 1963; Ehhalt and Haumacher, 1970).

(ii) Fewer constraints on the reverse troposphere-to-stratosphere transport into the LMS are available. The existence of this transport channel is well-proven (Kritz et al., 1991; Boering et al., 1995; Dessler et al., 1995; Hintsa et al., 1998; Lelieveld et al., 1997; Ovarlez et al., 1999; Ray et al., 1999). More recent aircraft data suggest a mixing layer just above the extratropical tropopause in which in-mixed tropospheric air mixes with descending lower stratospheric air (Bujok, 1998; Fischer et al., 2000; Rood et al., 2000; Zahn, 2001; Hoor et al., 2002). The presence of such a mixing layer is compatible with findings derived from model calculation (Chen, 1995; Eluskiewicz, 1996) and meteorological analyses (Dethof et al., 2000) which infer vital year-around bi-directional cross-tropopause transport below a potential temperature iso-surface of 340 K. The latter studies forecast stronger extratropical troposphere-to-stratosphere transport in summer, in contrast to ozone data collected by ozone sondes and on satellite (Rood et al., 2000) who derive stronger cross-tropopause mixing in winter and spring, and analyses based on UKMO meteorological data by Seo and Bowmann (2001) who found greatest upward transport into the LMS in fall and winter. Besides this qualitative picture, no consolidated quantitative numbers about tracer and mass fluxes into the LMS are available. The same applies for the influence of sporadic deep-convection events into the LMS, also proven to exist (Hauf et al., 1995; Poulida et al., 1996; Fischer et al., 2003).

(iii) After studies focusing on the radioactive fallout following the stratospheric bomb tests in the 50s and 60s (e.g. Junge, 1963; Ehhalt and Haumacher, 1970), recent studies using meteorological analyses again focus on the geographical distribution of downward and upward transport across the tropopause (Wernli et al., 2002; Sprenger

and Wernli, 2003, Stohl et al., 2003). These studies suggest considerable longitudinal, latitudinal, and inter-hemispheric asymmetries, in the northern hemisphere with peaking exchange in the Atlantic and Pacific storm track regions. However, no consistent, quantitative, and 3-dimensional illustration of downward and upward transport across the extratropical tropopause is available to date.

In this paper, co-variations of O_3 and CO just above the extratropical tropopause are analysed in respect of cross-tropopause tracer transport. The tracer-tracer correlation technique applied has been deployed with success for identifying mixing processes in the winter polar stratosphere (Waugh et al., 1997; Plumb et al., 2000) and was lately adopted to the tropopause region (Bujok, 1998; Fischer et al., 2000; Hoor et al., 2002).

The O_3 and CO data analysed here were collected during the passenger aircraft project CARIBIC in the years 1997 to 2002. In Part I of this study (Passenger aircraft project CARIBIC 1997–2002, Part I: the extratropical chemical tropopause), the O_3 and CO data are used to define a chemical tropopause in the extratropics. In this part can also be found (i) details about the flight statistics and the meteorological conditions along the chosen three CARIBIC flights routes (Germany to the Indian Ocean, southern Africa, and the Caribbean), (ii) a description of the O_3 and CO instruments, and (iii) importantly, a comprehensive description of the processes controlling the relationship of O_3 and CO in the upper troposphere/lower stratosphere (UTLS).

The paper is arranged as follows: first, the downward transport of O_3 is studied using comparisons of the seasonal variations of O_3 recorded during CARIBIC at 9–12 km (i) with those observed by ozone sondes at Hohenpeissenberg (Germany) and (ii) with PV data provided by the ECMWF. Second, the upward transport into the LMS is investigated based on the CARIBIC CO data in the LMS and seasonal variations of the O_3-CO relationship above the tropopause. Finally, the net cross-tropopause transport of O_3 is estimated and implications of the presented findings on the ventilation of the LMS are discussed.

2 Comparison with vertical ozone soundings

In Fig. 1 the seasonal variation of O_3 observed during CARIBIC at 9–12 km is compared with O_3 sonde data collected in the UTLS over Hohenpeissenberg (Germany, 48° N, 11° E). The CARIBIC O_3 data are displayed versus the potential vorticity (PV) which constitutes a vertical coordinate in the LMS; these data cover the upper troposphere and the lowest 2.0–2.5 km of the LMS. The Hohenpeissenberg data are plotted relative to the thermal tropopause and reach another 3.0–3.5 km, i.e. together 6 km into the LMS. Over the altitude range covered by both data sets, close agreement is manifest (compare also with Fig. 6). This not self-evident finding demonstrates that the O_3 concentration in the LMS is primarily determined by the distance above the tropopause and the time in the year. The dependence on sampling location is comparatively weak, in agreement with Logan (1999a, b).

The O_3 maximum shifts from February/March in the stratospheric overworld by 3.5 months to June at the tropopause (Fig. 1d). At first sight, both data sets seem to simply illustrate the descent of O_3 from the stratospheric overworld through the LMS into the troposphere. However, this is only part of the truth. A major objective of the present paper is to demonstrate that the obvious, towards the tropopause increasing phase shift is not alone due to the descent of O_3 through the LMS but is significantly modified due to dilution by in-flowing O_3-poor tropospheric air. Note, this inflow of tropospheric air is the only process that can explain the relative O_3 poorness and CO richness of the LMS (see Sect. 3 of Part I). Before discussing this troposphere-to-stratosphere transport in detail (Sect. 4), we will first derive some further constraints on the seasonal cycle of the downward transport of stratospheric O_3.

3 Co-variations between O_3 and PV

Both O_3 and PV constitute tracers of stratospheric air. Their well-known correlation in the LS, more specifically the constant slope and large positive correlation coefficient,

should thus characterise the downward O_3 transport from the overworld. We will now assess the slope dO_3/dPV and not the ratio O_3/PV in order to get rid of the significant, possibly varying contributions of tropospheric O_3. The slope dO_3/dPV observed during CARIBIC in the LMS (Fig. 2) undergoes an extreme seasonal variation having a maximum of 50–90 ppbv/PVU in April and a minimum of ∼10 ppbv/PVU in October. A sine variation that parameterise the O_3 data with PV > 1.5 PVU best, is also indicated. It maximises around 15 April and minimises 6 months later around 15 October. Without affecting the phase, the slope increases when penetrating deeper into the stratosphere (i.e. when considering only PV values larger than 2.5 and 3.5 PVU) because of a declining influence of tropospheric air.

A similar seasonal variation was found (i) by Roelofs and Lelieveld (2000, Table 1) using the MOZAIC data, which however peaked ∼10 days earlier (∼5 April) and showed higher O_3/PV slopes of on average 55 ppbv/PVU due to the slightly higher sampling altitude (dashed line in Fig. 2), and (ii) by Beekmann et al. (1994, Table 2). The maximum of dO_3/dPV just above the tropopause thus is by 6–8 weeks earlier in the year when compared to the seasonal O_3 variation at the tropopause, which peaks in June (Fig. 1d). As the seasonal variation of dO_3/dPV traces the downward transport of stratospheric ozone, this observation suggests that the peak in stratospheric ozone reach the tropopause already in April. The delayed O_3 maximum observed at the tropopause in June should hence be due to in-mixing of tropospheric air. This troposphere-to-stratosphere transport is studied next.

4 In-flow of tropospheric air into the LMS

With respect to the large O_3 variations and short transport times (weeks), ozone is a quasi-inert transport tracer in the LMS with a chemical lifetime exceeding one year (Solomon et al., 1985). Indeed, outflow of O_3-depleted air from the polar vortex did not influence the seasonal variation of O_3 over Hohenpeissenberg, as follows from the zero temporal trend of the phase of the seasonal O_3 variation between the beginning (1967)

and the end (2000) of the Hohenpeissenberg data set. Also the chemical O_3 production rates are negligible in the LMS (in contrast to the stratospheric overworld where the time scales for O_3 chemistry and transport can be of the same order, Fahey and Ravishankara, 1999).

Therefore, the stratospheric overworld constitutes the sole major ozone source for the LMS. At the upper entrance to the LMS, i.e. the 380–400 K θ-surface, the seasonal amplitude of O_3 amounts to only 10% of the annual mean (Fig. 1d). Towards the tropopause this seasonal amplitude intensifies to ∼40%, both when displaying the data relative to the thermal tropopause (Fig. 1d) and relative to isentropic surfaces (Fig. 1e). Such an intensification of the seasonal O_3 variation towards the tropopause was also found by Rood et al. (2000). If this growing seasonal amplitude at a certain station would only be due to downward propagation of O_3 from the overworld, quite extensive horizontal re-distribution of O_3 must exist within the LMS in association with different seasonal O_3 variations at other stations. This is not consistent with observations. Logan (1999a, b) demonstrated that the observed seasonal variation is a prominent feature existing throughout the northern hemispheric lowermost stratosphere, with only a weak latitudinal and longitudinal phase shift. It is also clear that a seasonal change in the velocity of downward O_3 transport cannot cause such an increasing seasonal variation towards the tropopause.

The only remaining explanation of the increasing seasonal O_3 amplitude towards the tropopause is in-flow of O_3-poor tropospheric air. This in-flow should reach its maximum impact in autumn in order to explain the low O_3 levels in the LMS in that season. In fact, this hypothesis is supported by a number of other studies. For instance, based on SAGE II H_2O and O_3 observations, Pan et al. (1997) and Wang et al. (1998) identified isentropic in-flow of tropospheric air as a major process controlling the seasonal H_2O and O_3 cycle in the LMS. Using balloon-borne CFC and H_2O observations at 35° N, Ray et at. (1999) showed that in September the LMS contains 60–90% tropospheric air quasi-isentropically mixed-in, but in May only 10–20%. Ovarlez et al. (1999) found maximum impact of water vapour from the troposphere in summer. Also model calcu-

lations by Chen (1995) and Eluskiewicz (1996) forecast maximum quasi-isentropic flow into the LMS in summer with a corresponding time lag in the species concentrations.

This in-flow of tropospheric air into the LMS is also traced by the CO data gathered during CARIBIC (Fig. 3). CO decreases from 70–100 ppbv at the tropopause to 35–40 ppbv at PV=8–9 PVU, i.e. 2.0–2.5 km above the tropopause. Consider that the local chemical equilibrium level in the LMS is 10–20 ppbv only (see Sect. 3 in Part I). Moreover, CO undergoes a clear seasonal variation in the LMS, with a gradual phase shift with altitude above the tropopause. CO maximises in April in the UT (see also Zahn et al., 2002) and at the tropopause, but in mid-summer at PV ≈8 PVU, i.e. ∼2 km above the tropopause. This gradual phase shift with altitudes can be explained by the increasing impact of in-flowing CO-rich tropospheric air at higher potential temperatures (lower latitudes), which was shown to maximise in summer (see Introduction).

5 The extratropical tropopause mixing layer

The mixing line concept presented in Sects. 3 and 4 in Part I will now be applied to infer further constraints on the extratropical tropopause mixing layer and quasi-isentropic troposphere-to-stratosphere transport. As an example, Fig. 4 shows the O_3-CO relationship recorded during four typical flights in different seasons. In autumn/winter the mixing line is located distinctly further left in the O_3-CO plot than in spring/summer. This seasonality must be due to a seasonal variation of the trace gas compositions of the two mixing reservoirs, that are "midlatitude UT air" and "unperturbed LMS air". These are the end points of the mixing lines (squares) in Fig. 4. The seasonal variations of these reservoirs are inferred simply by plotting their O_3 and CO mixing ratios, being for the upper troposphere O_3(UT) and CO(UT), and for the LMS O_3(LMS) and CO(LMS), for each flight versus time of the year. Three of the four seasonal cycles can be well-approximated by sine curves. They are schematically indicated in the outer grey frame of Fig. 4 and explicitly listed in Table 1.

O_3(UT) is by definition identical with $O_3(TP_{chem})$ (Eq. 1 in Part I). The seasonal variation of CO(UT) along the CARIBIC flight routes was derived in Zahn et al. (2002) (see also Fig. 3). It maximises around 1 April and minimises 6 months later with an amplitude of ∼10 ppbv. Unfortunately, the CARIBIC aircraft rarely crossed the mixing layer upper border, so that the seasonal variation of CO(LMS) could not accurately be derived. However, as seen in Fig. 4, the seasonal variation of CO(LMS) is apparently small. Hence, CO(LMS) is simply set to a constant value of 38 ppbv, that is the annual mean CO mixing ratio at PV=8–9 PVU. O_3(LMS) is then estimated by plotting the O_3 mixing ratio at this constant value $CO(LMS)|_{mean}$ (Fig. 3) versus season (Fig. 5). This simplification has little influence on the phase and amplitude of the inferred seasonal variation of O_3(LMS), because of the flatness of the mixing lines (Fig. 4) and the weak seasonal variation of CO(LMS) (Fig. 3 and Hoor et al., 2002) relative to the total vertical gradient, CO(UT)-CO(LMS). O_3(LMS) is in phase with $O_3(TP_{chem})$ with an annual mean of 360 ppbv (Table 1), although the Hohenpeissenberg O_3 data suggest a clear phase shift with altitude (Fig. 1). This apparent discrepancy is most likely associated with the fact that the CARIBIC aircraft sampled stratospheric air almost exclusively around tropopause fold structures (Sect. 2 of Part I), where the air in the upper part of the mixing layer may have a different origin and thus different seasonal phase compared to the air in the lower part of the mixing layer.

Finally, the thickness of the extratropical tropopause transition layer is estimated by comparing the seasonal O_3 variation observed during CARIBIC with the Hohenpeissenberg O_3 data at different distances above the thermal tropopause (Fig. 6). This comparison indicates that the mixing layer probed during CARIBIC or at least its well-ventilated part that is characterised by a straight mixing line, showed a quite constant vertical extension of ∼2 km throughout the year.

Orvalez et al. (1999) and Hoor et al. (2002) in contrast suggested that the mixing layer embraces a distinctly larger potential temperature range in summer (∼40 K) compared to winter (∼20 K). This difference to our finding cannot be assigned to the discussed undersampling of the mixing layer upper part by CARIBIC, i.e. the large uncertainty of CO(LMS), due to the weak influence of variations in CO(LMS) on the

interference of O_3(LMS), see above. This difference may be attributed to the peculiar meteorological conditions present when the CARIBIC aircraft probed stratospheric air (Sect. 2 of Part I). It should also be considered that the mixing layer most likely has a "smooth" upper border, i.e. has a well-ventilated lower part and a successively less well-ventilated upper part that is increasingly impacted by tropospheric in-flow at higher potential temperatures or lower latitudes, respectively.

6 Estimate of the downward cross-tropopause flux of stratospheric ozone

We observed considerable seasonal O_3 variations at the chemical tropopause (Fig. 5 in Part I), the dynamical tropopause (Fig. 6 in Part I) and in the LMS (Fig. 1). In the latter sections it was demonstrated that these seasonal O_3 variations are primarily of dynamical nature, namely caused by mixing of descending O_3-rich stratospheric air with ascending O_3-poor tropospheric air.

Starting from the overworld, the O_3 mixing ratio steadily decreases towards the tropopause (Fig. 1), due to increasing contribution of tropospheric air. However, the seasonal amplitude of O_3 relative to the annual mean at a certain distance above the tropopause should more or less be conserved, because of the short transport time scales and the comparably weak seasonal cycle of O_3 in the tropospheric air. This is indeed so. Using the Hohenpeissenberg data (Fig. 6), the amplitude ratio O_3^{max} (in May)/O_3^{min}(in November) at certain distances above the tropopause (ΔH^{TP}) is 515 ppbv/252 ppbv≈2.04 at ΔH^{TP}=2.0 km, 425 ppbv/188 ppbv≈2.26 at ΔH^{TP}=1.0 km, 319 ppbv/146 ppbv≈2.18 at ΔH^{TP}=0.6 km, 241 ppbv/118 ppbv≈2.04 at ΔH^{TP}=0.3 km, 179 ppbv/90 ppbv≈1.99 at ΔH^{TP}=0 km.

In other words, all stratospheric O_3 entering the mixing layer through its upper boundary will in the order of weeks end up in the troposphere. This is an one-way transport. It allows us to roughly estimate the net cross-tropopause flux of stratospheric O_3, j^{TP}_{ozone}. It is a product of the initial O_3 volume mixing ratio before mixing starts, i.e. that at the

top of the mixing layer $[O_3]_{LMS}$, and the net cross-tropopause mass flux:

$$j^{TP}_{ozone} = [O_3]_{LMS} \cdot j^{TP}_{mass} \quad (1)$$

The annual mean value $< [O_3]_{LMS} >$ observed during CARIBIC and over Hohenpeissenberg is ∼360 ppbv (Table 1). The mass flux j^{TP}_{mass} is the sum of (i) the net downward mass flux across the LMS upper boundary, the 380 K surface, $j^{380\,K}_{mass}=(2.4–5.0)\cdot 10^{17}$ kg yr^{-1} for the northern hemisphere (Rosenlof and Holton, 1993; Appenzeller et al., 1996; Juckes, 1997; Gettelman and Sobel, 2000; Olsen et al., 2002), and (ii) the in-flux of tropospheric air into the LMS along isentropic surfaces located above the aircraft, i.e. between 380 K and ∼310 K in winter and ∼330 K in summer, respectively. The latter is assumed to be distinctly smaller than $j^{380\,K}_{mass}$ (Sprenger and Wernli, 2003) and will be neglected for this estimate. Using these numbers, a net NH cross-tropopause O_3 flux of 145–300 Tg O_3 yr^{-1} or $(2.2–4.7)\cdot 10^{10}$ O_3-molecules cm^{-2} s^{-1} is inferred, which is a lower limit and indeed falls well within the lower range of other estimates (Murphy and Fahey, 1994; Gettelmann et al., 1997; Tie and Hess, 1997; Lamarque et al., 1999; Lelieveld and Dentener, 2000; McLinden et al., 2000; Olsen et al., 2001, 2002, and references therein).

Besides this estimate of the annual mean flux, the data provide constrains on the phase and the amplitude of j^{TP}_{ozone}. $j^{380\,K}_{mass}$ is estimated to peak around 1 January exceeding the minimum six months apart by a factor of 2.5–3.0 (Appenzeller et al., 1996). $[O_3]$ at the upper boundary of the mixing layer, $[O_3]_{LMS}$, and in the entire mixing zone peaks around 1 May exceeding the minimum in November by a factor of ∼2.1 (see above). As explained above, the observed ozone maximum around 1 May is not exactly in-phase with the downward transport of stratospheric ozone, but slightly phase-shifted due to in-mixing of tropospheric air. As shown in Fig. 2 (and the relevant discussion in Sect. 3), the net cross-tropopause transport of O_3 is assumed to peak two weeks earlier in the year, i.e. around 15 April.

Assuming that the downward transport within the LMS (i) is indeed one-way, i.e. do not alter much the amplitude of the seasonal variation of the net air mass flux with

altitude, and (b) the flux maximum is around 15 April (instead of 1 May). Then, by applying Eq. 1 (with shifting the phase by 2 weeks forward), the seasonal peak-to-peak value of net cross-tropopause O_3 transport is estimated to ∼6, in agreement with the only previous observational estimate by Danielsen and Mohnen (1977), see Fig. 7. The seasonal variation of net downward cross-tropopause O_3 flux can then be parameterised as:

$$j^{TP}_{ozone} = 3.4 + 2.4 \cdot \sin[2\pi \cdot (\text{doy} - 15)/365] \quad (2)$$

in 10^{10} molecules $cm^{-2}\,s^{-1}$. Considering the restricted dataset available as well as the assumptions and simplifications included, the magnitude as well as amplitude and phase of this estimate agree surprisingly well with other observational and model estimates. Its uncertainty is affected by the uncertainty of the validity of the formalism applied, and depends on the representativeness of the included O_3 data for the rest of the northern hemisphere.

7 Implications for processes causing STE

Finally we discuss the above findings in light of the current knowledge about extratropical troposphere-stratosphere exchange.

(i) Besides net downward transport across the extratropical tropopause, active gross (bi-directional) isentropic exchange occurs throughout the year. However, only little of the upward moving tropospheric air penetrates deep into the lowermost stratosphere. Rather, a well-ventilated mixing layer is formed just above the tropopause where the injected tropospheric air is mixed with subsiding lower stratospheric air. This view supports many other observations, e.g. (Bujok, 1998; Lelieveld et al., 1997; Rood et al., 2000, Fischer et al., 2000; Hoor et al., 2002), and conclusions from meteorological analyses (e.g. Dethof et al., 2000; Wernli and Bourqui, 2002; Stohl et al., 2003). The lower and preponderant part of the mixing lines is linear (see Hoor et al., 2002,

and Fig. 4), indicating that the time scale for mixing is shorter than the local chemical lifetime of the considered tracers. The chemical lifetime of CO for instance is ∼2 months in summer. The weak vertical phase shift of the seasonal O_3 variation above the tropopause (Fig. 1) likewise demonstrates that the turnover time of the mixing layer is no longer than some weeks. The existence of such a well-ventilated layer has crucial implications for the chemistry in the UTLS region, in particular with respect to changing aircraft emissions and changing chemical composition of the troposphere.

(ii) The O_3-CO relationship above the tropopause reflects the partitioning between tropospheric air (traced by CO) and stratospheric air (traced by O_3). Its property (compactness, variability, seasonality) places constraints on the nature and magnitude of the processes that cause the final irreversible mixing between tropospheric and stratospheric air. During all flights, the correlation between O_3 and CO above the tropopause was compact (comparable to the flights exhibited in Fig. 4). A prerequisite for the existence of such compact relationships is that stirring along isentropic surfaces strongly exceeds mixing across isentropes (diabatic transport), as shown for mixing processes near the stratospheric polar vortex (Plumb et al., 2000, and references therein). The invariable compactness of the tracer-tracer correlations observed during CARIBIC thus demonstrates that midlatitude STE primarily occurs along isentropic surfaces and that short-term processes such as sporadic deep convection of lower tropospheric air across the tropopause, although proven to exist (Poulida et al., 1996; Waibel et al., 1999; Fischer et al., 2002), is of minor importance for the ventilation of the lowermost stratosphere.

(iii) Another constraint is provided by the surprisingly small short-term scatter of the seasonal O_3 variation at the tropopause (Fig. 5 in Part I) and of the mixing lines above it (Fig. 5), encountered during the sporadic CARIBIC probes. It reveals that the extratropical tropopause mixing layer is not formed by individual mixing events near the actual sampling location, but rather due to a superposition of many cross-tropopause mixing events occurring largely remote from the sampling location. It also denotes that extratropical net as well as gross STE is not controlled by the local instantaneous me-

teorological situation at the tropopause, e.g. by the frequency or strength of tropopause folds, since these features vary in occurrence and intensity day-by-day and throughout the year (Sprenger et al., 2003). Therefore, tropopause features ranging from mesoscale tropopause folds to small-scale filaments seem to act primarily as "valves" that enable net and gross cross-tropopause exchange, but that regulate only to a minor degree the amount of air transferred. This stands in excellent agreement with theoretical considerations by Haynes et al. (1991) and Holton et al. (1995), who explain STE as part of the general atmospheric circulation primarily controlled by wave-induced forces in the stratosphere.

(iv) Our observations suggest maximum downward cross-tropopause flux of ozone in April (Fig. 7), in reasonable agreement with other observational and theoretical studies (Danielsen and Mohnen, 1977; Beekman et al., 1994; Menzies and Tratt, 1995; Appenzeller et al., 1996; Seo and Bowman, 2001). This maximum cross-tropopause O_3 flux has a time lag of about three months relative to the major downward O_3 in-flux from the overworld at 380 K or ∼100 hPa. The low wintertime O_3 concentration at and above the extra-tropical tropopause further demonstrates that downward flux of stratospheric ozone is weak in mid-winter. Consider however, that the cross-tropopause mass flux apparently shows a quite different seasonal variation. The Lagrangian trajectory models Lagranto and Flexpart predict the maximum stratosphere-to-troposphere flux for winter and the minimum for summer (Sprenger et al., 2003; Stohl et al., 2003, and references therein).

In summary, the lowermost stratosphere can be viewed as a variable buffer reservoir or "bellows", furnished with two "valves", one at the top, the 380–400 K θ-surface, and one at the bottom, the tropopause. In late autumn/winter, the lowermost stratosphere is inflated by overworld air via the upper valve (opened by breaking Rossby waves and strong diabatic subsidence) to achieve its maximum mass in January (being for the NH ∼37% larger than its minimum mass in August; Appenzeller et al., 1996), the "inhaling effect". At the same time, the lower valve remains largely closed, because of the strong PV gradient along the θ-surfaces crossing the tropopause (Haynes and Shuckburgh,

2000), the "transport barrier effect". Bi-directional cross-tropopause transport near the polar jet occurs (Dethof et al., 2000; Wernli and Bourqui, 2001; Seo and Bowman, 2002), i.e. at isentropic surfaces below ∼320 K, but this exchange is presumably shallow and will not result in significant net tracer exchange. Towards spring/summer, the upper valve is shut, whilst the tropopause becomes increasingly permeable because of a weakening transport barrier effect. Air from the shrinking lowermost stratosphere flows into the troposphere mainly in spring. In summer, i.e. after the "squeezing out" of the lowermost stratosphere, the weakness of the transport barrier, especially near the Indian and Mexican monsoon regions (Chen, 1995), enables deeper entrainment of tropospheric air into the lowermost stratosphere also at isentropic surfaces above ∼320 K, in agreement with observations (Ray et al., 1999) and model results (Chen, 1995; Eluskiewicz et al., 1996; Dethof et al., 2000). Note that the seasonal amplitude of the tracer (O_3) cross-tropopause flux surpasses that of the mass flux, because of (i) the replenishment of the lowermost stratosphere by tracer-rich overworld air before its outflow into the troposphere, and (ii) the seasonally varying in-flow of (O_3-poor) tropospheric air. That is, the O_3 minimum occurring in autumn anyway is intensified by in-flowing tropospheric air. Still in winter and early spring the lower part of the LMS, i.e. the tropopause transition layer, contains large contributions of tropospheric air, before the peaking O_3 levels from the overworld reach the mixing layer around April and the major O_3 export into the troposphere starts. Admittedly, this description of STE is figurative, but it does characterise the processes associated with STE in a quite appropriate manner.

8 Conclusions

In Part II of this study, the CARIBIC O_3 and CO data were analysed in respect of tracer transport around the tropopause and in the lowermost stratosphere (LMS). The major finding were inferred from the seasonal variations of the two tracers relative to the tropopause, by interpreting observed co-variations between O_3 and CO, and by

comparisons with ozone sonde data over Hohenpeissenberg.

In agreement with other studies, e.g. Logan (1999a, b), considerable sine seasonal variation of ozone at the tropopause and in the LMS was observed, with a maximum in April/May and a minimum six months later in October/November. This seasonality is explained by a superposition of the seasonal variation of descending stratospheric air which results in peaking O_3 mixing ratios in April at the tropopause and isentropic in-flux of O_3-poor tropospheric air into the LMS which causes a time lag towards summer that continuously increases towards the tropopause.

As demonstrated previously (Bujok, 1998; Fischer et al., 2002; Hoor et al., 2002), this isentropic in-flow of tropospheric air causes a tropopause transition layer, i.e. a mixing layer in which descending stratospheric air and ascending tropospheric air mix. The chemical composition of the tropopause mixing layer shows a continuous transition from the one of upper upper tropospheric air to the one of unperturbed lowermost stratospheric air. Its turnover time is in the order of weeks estimated on the basis of the vertical profile of the seasonal O_3 variation in the LMS (Fig. 6) and the observed compact linearity among O_3 and CO (Fig. 4). Following Mahlmann et al. (1986), Plumb and Ko (1992), and Waugh et al. (1997), the linearity of a tracer-tracer relationship in the stratosphere marks a mixing process that primarily occurs along isentropic surfaces and that is faster than the chemical processing of the considered tracers. The local chemical lifetime of CO is only about two months in summer, and thus the turnover time of the tropopause mixing layer shorter than this.

Importantly, the observed O_3-CO mixing lines above the tropopause are not formed by single mixing events, but by a superposition of a large number of individual mixing events, which together maintain the well-ventilated tropopause transition layer. Its spatial variability is assumed to be small. This finding is based on the observed surprisingly weak short-term variability of the O_3-CO relationship above the tropopause, i.e. its only weak influence from the instantaneous synoptic condition during sampling. This implies that net as well as gross cross-tropopause tracer exchange is not controlled by local processes, i.e. the instantaneous synoptic condition, but is determined by large-

scale slowly varying processes. Indeed, the short-term variability of the mixing layer is weak, but it undergoes a gradual and strong seasonal variation. Our data thus provide observational evidence for theoretical studies by Haynes et al. (1991) and Holton et al. (1995) who explain stratospheric-troposphere exchange as part of the global-scale circulation that is largely driven by wave-induced forces in the stratospheric overworld.

The weak spatial variability of the mixing layer even allowed us to infer an estimate on the downward flux of stratospheric ozone into the troposphere by using the sporadic CARIBIC samplings in the mixing layer. Integrating vertical O_3 sonde data over Hohenpeissenberg (48° N, 11° E), it is shown that the downward transport of O_3 through the mixing layer can be described as 1-dimensional downward flux. Assuming a reasonable stratosphere-to-troposphere mass flux, a downward net cross-tropopause O_3 flux of $3.4 + 2.4 \cdot \sin[2\pi \cdot (\mathrm{DayOfYear} - 15)/365]$ 10^{10} molecules $\mathrm{cm}^{-2}\,\mathrm{s}^{-1}$ is estimated as a lower limit. Indeed, this number falls in the lower range of other estimates.

One focus of the new CARIBIC flight phase starting in May 2004 will be a more detailed picture of the extratropical tropopause transition layer by including further tracers such as NO_y or water vapour.

Acknowledgements. The CARIBIC project is supported by the European Union (grant ENV4-CT95-0006 and EVK2-2001-00007), and the German Ministry for Education and Research (BMBF, AFO 2000), Ford Research, and Ruhrgas AG. We thank LTU-International Airways (Düsseldorf) for their support and H. Claude (DWD) for providing the O_3 sonde data collected at Hohenpeissenberg.

References

Appenzeller, C., Holton, J. R., and Rosenlof, K. H.: Seasonal variation of mass transport across the tropopause, J. Geophys. Res., 101, 15 071–15 078, 1996.

Beekmann, M., Ancellet, G., and Mégie, G.: Climatology of tropospheric ozone in southern Europe and its relation to potential vorticity, J. Geophys. Res., 99, 12 841–12 853, 1994.

Boering, K. A., Hintsa, E. J., Wofsky, S. C., Anderson, J. G., Daube Jr., B. C., Dessler, A. E., Loewenstein, M., McCormick, M. P., Podolske, J. R., Weinstock, E. M., and Yue, G. K.:

Measurements of stratospheric carbon dioxide and water vapor at northern midlatitudes: Implications for troposphere-to-stratosphere transport, Geophys. Res. Lett., 22, 2737–2740, 1995.

Bujok, O.: In-situ measurement of long-lived trace gases within the lowermost stratosphere: Development and application of an airborne gaschromatographic detection method, PhD thesis (in German), Forschungszentrum Jülich, Institute of chemistry and dynamics of the geosphere, Rep. Jül-3517, 1–202, 1998.

Chen, P.: Isentropic cross-tropopause mass exchange in the extratropics, J. Geophys. Res., 100, 16 661–16 673, 1995.

Danielsen, E. F. and Mohnen, V. A.: Project Duststorm Report: Ozone transport, in situ measurements and meteorological analyses of tropopause foldings, J. Geophys. Res., 82, 5867–5877, 1977.

Dessler, A. E., Weinstock, E. M., Anderson, J. G., and Chan, K. R.: Mechanisms controlling water vapor in the lower stratosphere: A tale of two stratospheres, J. Geophys. Res., 100, 23 167–23 172, 1995.

Dethof, A., O'Neill, A., and Slingo, J.: Quantification of isentropic mass transport across the dynamical tropopause, J. Geophys. Res., 105, 12 279–12 293, 2000.

Eluskiewicz, J.: A three-dimensional view of the stratosphere-to-troposphere exchange in the GFDL SKYHI model, Geophys. Res. Lett., 23, 2489–2492, 1996.

Emmons, L. K., Hauglustaine, D. A., Müller, J.-F., Carroll, M. A., Brasseur, G. P., Brunner, D., Staehelin, J., Thouret, V., and Marenco, A.: Data composites of airborne observations of tropospheric ozone and its precursors, J. Geophys. Res., 105, 20 497–20 538, 2000.

Ehhalt, D. H. and Haumacher, G.: The seasonal variation in the concentration of strontium 90 in rain and its dependence on latitude, J. Geophys. Res., 75, 3027–3031, 1970.

Fahey, D. W. and Ravishankara, A. R.: Summer in the stratosphere, Science, 285, 208–210, 1999.

Fischer, H., Wienhold, F. G., Hoor, P., Bujok, O., Schiller, C., Siegmund, P., Ambaum, M., Scheeren, H. A., and Lelieveld, J.: Tracer correlations in the northern high latitude lowermost stratosphere: Influence of cross-tropopause mass exchange, Geophys. Res. Lett., 27, 97–100, 2000.

Fischer, H., de Reus, M., Traub, M., Williams, J., Lelieveld, J., de Gouw, J., Warneke, C., Schlager, H. , Minikin, A., Scheele, R., and Siegmund, P.: Deep convective injection of boundary layer air into the lowermost stratosphere at midlatitudes Atmospheric Chemistry

and Physics, 3, 739–745, 2003.

Gettelmann, A. and Sobel, A. H.: Direct diagnoses of stratosphere-troposphere exchange, J. Atmos. Sci., 57, 3–16, 2000.

Gettelmann, A., Holton, J. R., and Rosenlof, K. H.: Mass fluxes of O_3, CH_4, N_2O, and CF_2Cl_2 in the lower stratosphere calculated from observational data, J. Geophys. Res., 102, 19 149–10 159, 1997.

Hauf, T., Schulte, P., Alheit, R., and Schlager, H.: Rapid vertical transport by isolated midlatitude thunderstorms, J. Geophys. Res., 100, 22 957–22 970, 1995.

Haynes, P. H. and McIntyre, M. E.: On the conservation and impermeability theorems for potential vorticity, J. Atmos. Sci., 47, 2021–2031, 1990.

Haynes, P. H., Marks, C. J., McIntyre, M. E., Sheperd, T. G., and Shine, K. P.: On the "downward control" of the extratropical diabatic circulations by eddy-induced mean zonal forces, J. Atmos. Sci., 48, 651–678, 1991.

Haynes, P. and Shuckburgh, E.: Effective diffusivity as a diagnostic of atmospheric transport, 2. Troposphere and lower stratosphere, J. Geophys. Res., 105, 22 795–22 810, 2000.

Hintsa, E. J., Boering, K. A., Weinstock, E. M., et al.: Troposphere-to-stratosphere transport in the lowermost stratosphere from measurements of H_2O, CO_2, N_2O, and O_3, Geophys. Res. Lett., 25, 2655–2658, 1998.

Holton, J. R., Haynes, P. H., McIntyre, M. E., Douglass, A. R., Rodd, R. B., and Pfister, L.: Stratosphere-troposphere exchange, Rev. Geophys., 33, 403–439, 1995.

Hoor, P., Fischer, H., Lange, L., Lelieveld, J., and Brunner, D.: Seasonal variations of a mixing layer in the tropopause region as identified by the CO-O_3 correlation from in-situ measurements, J. Geophys. Res., 107, doi:10.1029/2000JD000289, 2002.

Hoskins, B. J.: Towards a PV-theta view of the general circulation, Tellus, 43AB, 27–35, 1991.

Juckes, M.: The mass flux across the tropopause: quasi-geostrophic theory, Q.J.R. Meteorol. Soc., 123, 71–99, 1997.

Junge, C. E.: Air chemistry and radioactivity, International Geophysics Series, Vol. 4, Academic Press, New York, 238–281, 1963.

Kritz, M. A., Rosner, S. W., Danielsen, E. F., and Selkirk, H. B.: Air mass origins and troposphere-to-stratosphere exchange associated with midlatitude cyclogenesis and tropopause folding inferred from ^{7}Be measurements, J. Geophys. Res., 96, 17 405–17 414, 1991.

Lamarque, J.-F., Hess, P. G., and Tie, X. X.: Three-dimensional model study of the influence

of stratosphere-troposphere exchange and its distribution on tropospheric chemistry, J. Geophys. Res., 104, 26 363–26 372, 1999.
Lelieveld, J., Bregman, B., Arnold, F., Bürger, V., Crutzen, P. J., Fischer, H., Waibel, A., Siegmund, P., and van Velthoven, P. F. J.: Chemical perturbation of the lowermost stratosphere through exchange with the troposphere, Geophys. Res. Lett., 24, 603–606, 1997.
Lelieveld, J. and Dentener, F. J.: What controls tropospheric ozone?, J. Geophys. Res., 105, 3531–3551, 2000.
Logan, J. A.: An analysis of ozonesonde data for the troposphere: Recommendations for testing 3-D models and development of a gridded climatology for tropospheric ozone J. Geophys. Res., 104, 16 115–16 149, 1999a.
Logan, J. A.: An analysis of ozonesonde data for the lower stratosphere: Recommendations for testing models J. Geophys. Res., 104, 16 151–16 170, 1999b.
Mahlmann, J. D., Levy II, H., and Moxim, W.: Three-dimensional simulations of stratospheric N_2O: Predictions for other trace gases constituents, J. Geophys. Res., 91, 2687–2707, 1986.
Menzies, R. T. and Tratt, D. M.: Evidence of seasonally dependent stratosphere-troposphere exchange and purging of the lower stratospheric aerosol from a multiyear lidar data set, J. Geophys. Res., 105, 3139–3148, 1995.
McLinden, C. A., Olsen, S. C., Hannegan, B., Wild, O., Prather, M. J., and Sundet, J.: Stratospheric ozone in 3-D models: A simple chemistry and the cross-tropopause flux, J. Geophys. Res., 105, 14 653–14 665, 2000.
Murphy, D. M. and Fahey, D. W.: An estimate of the flux of stratospheric nitrogen and ozone into the troposphere, J. Geophys. Res., 99, 5325–5332, 1994.
Olsen S. C., McLinden, C. A., and Prather, M. J.: Stratospheric N_2O-NO_y system: Testing uncertainties in a three-dimensional framework, J. Geophys. Res., 106, 28 771–28 784, 2001.
Olsen, M. A., Douglass, A. R., and Schoeberl, M. R.: Estimating downward cross-tropopause ozone flux using column ozone and potential vorticity, J. Geophys. Res., 107, D22, 4636, doi:10.1029/2001JD002041, 2002.
Ovarlez, J., van Velthoven, P., and Schlager, H.: Water vapor measurements from the troposphere to the lowermost stratosphere: Some signatures of troposphere to stratosphere exchanges, J. Geophys. Res., 104, 16 673–16 678, 1999.
Pan, L., Solomon, S., Randel, W., Lamarque, J. F., Hess, P., Gille, J., Chiou, E. W., and McCormick, M. P.: Hemispheric asymmetries and seasonal variations of the lowermost strato-

spheric water vapor and ozone derived from SAGE II data, J. Geophys. Res., 102, 28 177–28 184, 1997.
Plumb, R. A. and Ko, M. K. W.: Interrelationships between mixing ratios of long-lived stratospheric constituents, J. Geophys. Res., 97, 10 145–10 156, 1992.
Plumb, R. A., Waugh, D. W., and Chipperfield, M.: The effects of mixing on tracer relationships in the polar vortices, J. Geophys. Res., 105, 10 047–10 062, 2000.
Poulida, O., Dickerson, R. R., and Heymsfield, A.: Stratosphere-troposphere exchange in a midlatitude mesoscale convective complex: 1. Observations, J. Geophys. Res., 101, 6823–6863, 1996.
Ray, E. A., Moore, F. L., Elkins, J. W., Dutton, G. S., Fahey, D. W., Vömel, H., Oltmans, S. J., and Rosenlof, K. H.: Transport into the Northern Hemisphere lowermost stratosphere by in situ tracer measurements, J. Geophys. Res., 104, 26 565–26 580, 1999.
Roelofs, G. J. and Lelieveld, J.: Model study of the influence of cross-tropopause O_3 transports on tropospheric O_3 levels, Tellus, 49B, 38–55, 1997.
Roelofs, G. J. and Lelieveld, J.: Model analysis of stratosphere-troposphere exchange of ozone and its role in the tropospheric ozone budget, in Chemistry and radiation changes in the ozone layer, edited by Zerefos, C. S., Isaksen, I. S. A., and Ziomass, I., Kluwer Academic Publishers, 25–43, 2000.
Roods, R. B., Douglass, A. R., Cerniglia, M. C., Sparling, L. C., and Nielsen, J. E.: Seasonal variability of middle-latitude ozone in the lowermost stratosphere derived from probability distribution functions, J. Geophys. Res., 105, 17 793–17 805, 2000.
Rosenlof, K. H. and Holton, J. R.: Estimates of the stratospheric residual circulation using the downward control principle, J. Geophys. Res., 98, 10 465–10 479, 1993.
Seo, K.-H. and Bowman, K. P.: A climatology of isentropic cross-tropopause exchange, J. Geophys. Res., 106, 28 159–18 172, 2001.
Solomon, S., Garcia, R. R., and Stordal, F.: Transport processes and ozone perturbations, J. Geophys. Res., 90, 12 981–12 989, 1985.
Sprenger, M. and Wernli, H.: A northern hemispheric climatology of cross-tropopause exchange for the ERA15 time period (1979–1993) J. Geophys. Res., 108, D12, 8521, doi:10.1029/2002JD002636, 2003.
Stohl, A., Wernli, H., Bourqui, M., Forster, C., James, P., Liniger, M. A., Seibert, P., and Sprenger, M.: A new perspective of stratosphere-troposphere exchange, Bull. Am. Met. Soc., doi:10.1175/BAMS-84-11-1565, 2003.

Tie, X. X. and Hess, P. G.: Ozone mass exchange between the stratosphere and the troposphere for background and volcanic sulfate aerosol conditions, J. Geophys. Res., 102, 25 487–25 500, 1997.

Waibel, A. E., Fischer, H., Wienhold, F. G., Siegmund, P. C., Lee, B., Ström, J., Lelieveld, J., and Crutzen, P. J.: Highly elevated carbon monoxide concentrations in the upper troposphere and lowermost stratosphere at northern midlatitudes during the STREAM II summer campaign, Chemosphere, Global Change Science, 1, 233–248, 1999.

Wang, P.-H, Cunnold, D., Zadowny, J., Pierce, R., Oltmans, J., Kent, G., and Steens, K.: Seasonal ozone variations in the isentropic layer between 330 and 380 K as observed by SAGE II: implications of extratropical cross-tropopause transport, J. Geophys. Res., 103, 28 647–28 659, 1998.

Waugh, D. W., Plumb, R. A., Elkins, J. W., et al.: Mixing of polar vortex air into middle latitudes as revealed by tracer-tracer scatter plots, J. Geophys. Res., 102, 13 119–13 134, 1997.

Wernli, H. and Bourqui, M.: A Lagrangian "1-year climatology" of (deep) cross-tropopause exchange in the extratropical Northern hemisphere, J. Geophys. Res., 107, D2, doi:10.1029/2002JD000812, 2002.

Zahn, A., Brenninkmeijer, C. A. M., Crutzen, P. J., Heinrich, G., Fischer, H., Cuijpers, J. W. M., and van Velthoven, P. F. J.: Distributions and relationships of O_3 and CO in the upper troposphere: The CARIBIC aircraft results 1997–2001, J. Geophys. Res., 107, D17, 4337, doi:10.1029/2001JD001529, 2002.

Table 1. Seasonal variations of CO and O_3 in midlatitude UT air and unperturbed LMS air which mix within the mixing layer above the tropopause.

	[CO] (ppbv)	[O_3] (ppbv)
UT	$94 + 10 \cdot \sin[2\pi \cdot (\text{doy}^{a} - 0)/365]^{b}$	$97 + 26 \cdot \sin[2\pi \cdot (\text{doy} - 30)/365]^{c}$
LMS	30–40	$360 + 130 \cdot \sin[2\pi \cdot (\text{doy} - 30)/365]$

[a] doy: day of year

[b] as shown by Zahn et al. (2002)

[c] identical with $O_3(TP_{chem})$ (Eq. 1 in Part I)

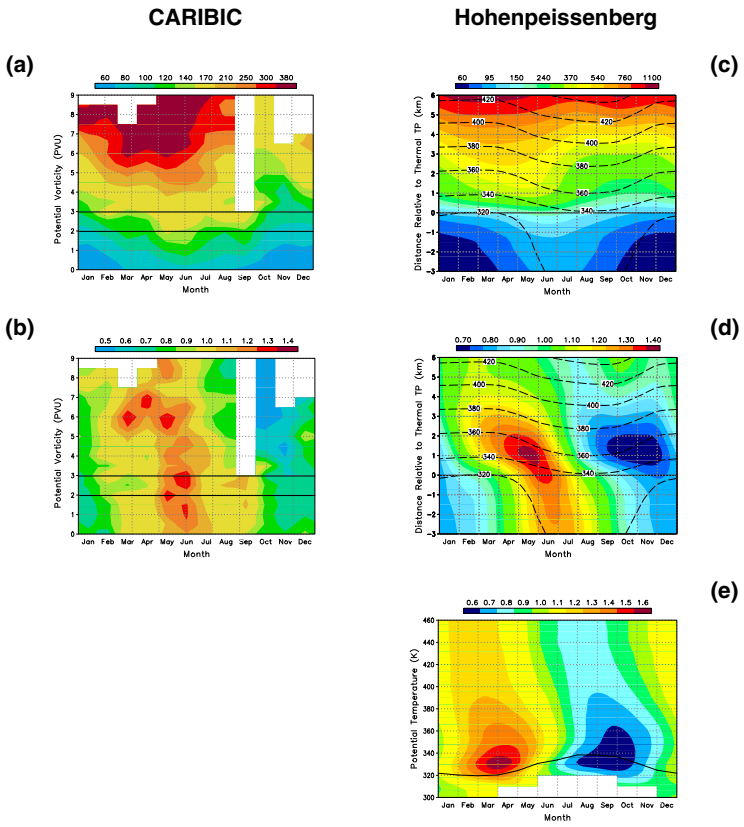

Fig. 1.

Fig. 1. Mean seasonal variation of ozone in the UTLS relative to the tropopause, left side: all CARIBIC data from 1997 to 2002, right side: Hohenpeissenberg O_3 soundings between 1967 and 2000, with courtesy of H. Claude (DWD, Hohenpeissenberg). Consider that the CARIBIC data reach only reach 2.0–2.5 km into the LMS, the Hohenpeissenberg data however reach 6.0 km into the LMS. The scales in the individuals graphs are chosen to illustrate the vertically changing seasonal variations of O_3 best. **(a)** O_3 (in ppbv) as function of the potential vorticity taken from ECMWF analysis. **(b)** Relative seasonal variation of O_3 at PV iso-surfaces. The two horizontal lines in (a) and (b) mark reasonable PV threshold values for the dynamical tropopause of 2 and 3 PVU. **(c)** O_3 (in ppbv) relative to the thermal tropopause. Dashed lines indicate potential temperature iso-surfaces. **(d)** Relative seasonal variation of O_3 at surfaces of constant distances relative to the thermal tropopause. **(e)** Relative seasonal variation of O_3 at potential temperature iso-surfaces. Graph (a) and (c) as well as (b) and (d) display the data exactly in the same manner; the only difference is that the Hohenpeissenberg data reach deeper into the LMS.

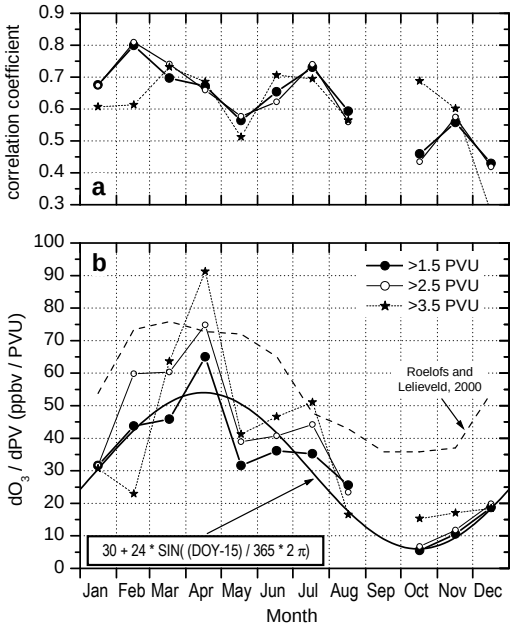

Fig. 2. Mean seasonal variation of the slope dO_3/dPV calculated for PV values larger than 1.5 PVU (dots), 2.5 PVU (circles), and 3.5 PVU (stars). All CARIBIC flights are considered. Dashed line indicates MOZAIC data published by Roelofs and Lelieveld (2000).

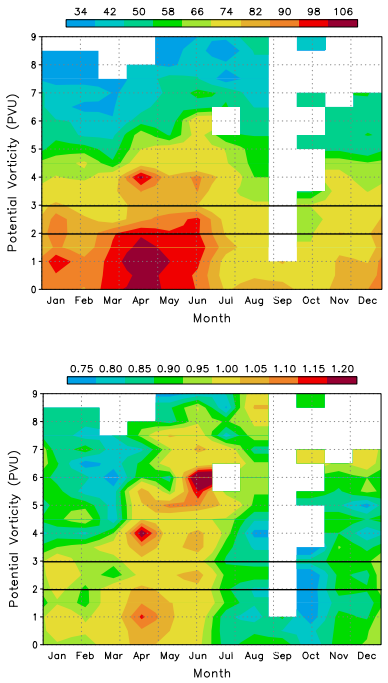

Fig. 3. Mean seasonal variation of CO in the UTLS measured during CARIBIC between 1997 and 2002, equivalent to Fig. 1a and b where the O_3 data are shown. **(a)** CO (in ppbv) as function of the potential vorticity taken from ECMWF analysis. **(b)** Same CO data as in (a), but plotted as relative variation in respect to the annual mean CO mixing ratio at the respective PV iso-surfaces. The two horizontal lines in (a) and (b) mark reasonable PV threshold values for the dynamical tropopause of 2 and 3 PVU.

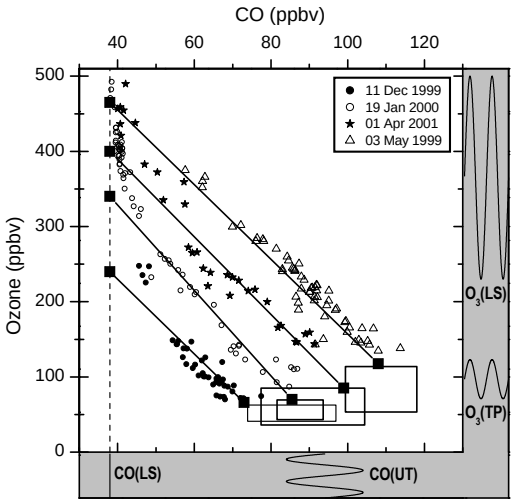

Fig. 4. Relationship between O_3 and CO observed in the LMS during four CARIBIC flights between December and May. For the tropospheric data of each flight a rectangle is depicted, whose dimensions in x- and y-direction are defined by the 1-σ variations of CO respectively O_3 of these data. The ends of each mixing line (straight lines) are indicated by squares. The seasonal variation at these ends in the UT and LMS are detailed in the outer grey frame as function of time. CO(LMS) is set to 38 ppbv as a first guess (see text). The other three seasonal variations were observed. All three can be well approximated by sine lines (see text).

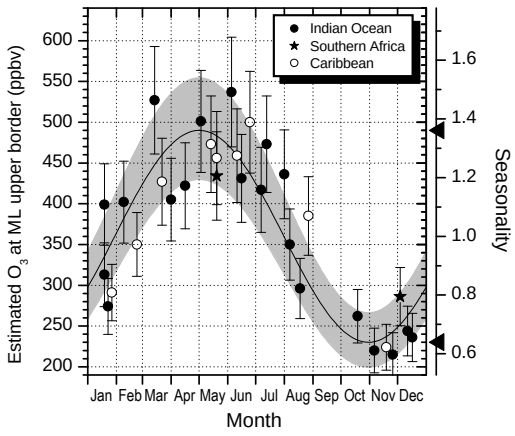

Fig. 5. Seasonal O_3 variation at CO=38 ppbv that roughly defines the mixing layer upper border, left y-axis as mixing ratio, and right y-axis as relative variation in respect to the annual mean of 360 ppbv, along the three CARIBIC flight routes (Fig. 1): Germany – Indian Ocean: full dots, Germany – Caribbean: open dots, Germany – southern Africa: stars. Because of the mostly small difference, for each outward and return flight only one data point is indicated. Sine line: seasonal variation that approximates the data best (as given in Table 1) with 1-σ scatter range (grey area).

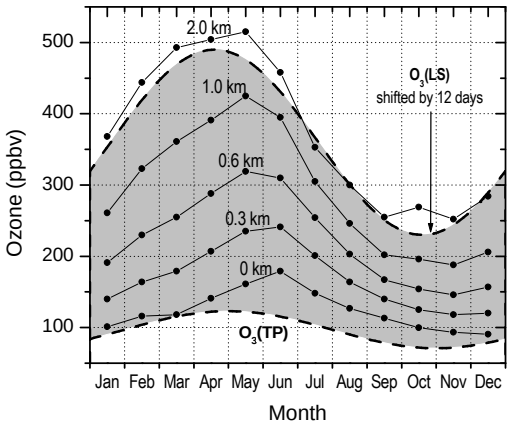

Fig. 6. Comparison of seasonal O_3 variation at different distances above the thermal tropopause observed over Hohenpeissenberg, with the ones recorded during CARIBIC at the chemical tropopause (lower dashed sine curve) and at the upper boundary of the mixing layer (upper dashed sine curve), both given in Table 1. The seasonal cycle of the latter has been forward-shifted by 12 days in order to achieve best agreement with the seasonal cycle of O_3 over Hohenpeissenberg 2 km above the thermal tropopause.

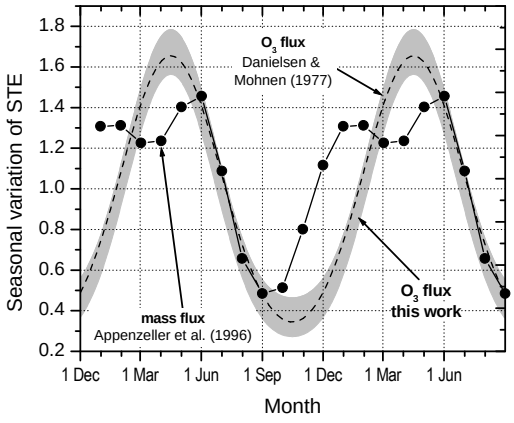

Fig. 7. Seasonal variation of net extratropical downward cross-tropopause flux, normalised to 1. The closed circles indicate the results of the mass flux calculation by Appenzeller et al. (1996) which only accounts for the seasonal change in volume of the lowermost stratosphere. The dashed line indicates the tracer (O_3, ^{90}Sr) flux inferred from observations after the atmospheric nuclear bomb tests in the 1950s and 1960s (Danielsen and Mohnen, 1977). The grey area gives the seasonal cycle of the O_3 flux including 1-σ deviation as derived from the CARIBIC data.